Monthly Notices
of the
ROYAL ASTRONOMICAL SOCIETY

MNRAS **483,** 2581–2591 (2019)
Advance Access publication 2018 December 6

doi:10.1093/mnras/sty3304

A remarkable change of the spectrum of the magnetic Of?p star HD 148937 reveals evidence of an eccentric, high-mass binary

G. A. Wade,[1]★ J. V. Smoker,[2] C. J. Evans,[3] I. D. Howarth,[4] R. Barba ,[5] N. L. J. Cox,[6,7] N. Morrell,[8] Y. Nazé ,[9] J. Cami,[10,11] A. Farhang,[10,12] N. R. Walborn,[13]† J. Arias[5] and R. Gamen[14]

[1]*Department of Physics & Space Science, Royal Military College of Canada, PO Box 17000 Station Forces, Kingston, ON K7K 0C6, Canada*
[2]*European Southern Observatory, Alonso de Cordova 3107, Casilla 19001, Vitacura, Santiago 19, Chile*
[3]*UK Astronomy Technology Centre, Royal Observatory, Blackford Hill, Edinburgh EH9 3HJ, UK*
[4]*Department of Physics & Astronomy, University College London, Gower Street, London WC1E 6BT, UK*
[5]*Departamento de Física y Astronomía, Universidad de La Serena, Av. Cisternas 1200, La Serena, Chile*
[6]*Anton Pannekoek Institute for Astronomy, University of Amsterdam, NL-1090 GE Amsterdam, The Netherlands*
[7]*ACRI-ST, 260 Route du Pin Montard, Sophia Antipolis, France*
[8]*Las Campanas Observatory, Carnegie Observatories, Casilla 601, La Serena, Chile*
[9]*FNRS - University of Liège, B5C, Allée du 6 Août 19c, B4000 Liège, Belgium*
[10]*Department of Physics and Astronomy and Centre for Planetary Science and Exploration (CPSX), The University of Western Ontario, London, ON N6A 3K7, Canada*
[11]*SETI Institute, 189 Bernardo Ave, Suite 100, Mountain View, CA 94043, USA*
[12]*School of Astronomy, Institute for Research in Fundamental Sciences, 19395-5531 Tehran, Iran*
[13]*Space Telescope Science Institute, 3700 San Martin Drive, Baltimore, MD 21218, USA*
[14]*Instituto de Astrofísica de La Plata, CONICET–UNLP and Facultad de Ciencias Astronómicas y Geofísicas, UNLP, Paseo del Bosque, s/n, La Plata, Argentina*

Accepted 2018 November 26. Received 2018 November 25; in original form 2018 April 10

ABSTRACT

We report new spectroscopic observations of the magnetic Of?p star HD 148937 obtained since 2015 that differ qualitatively from its extensive historical record of weak, periodic spectral variations. This remarkable behaviour represents clear evidence for an unprecedented change in the character of variability of the star. In this paper, we describe the new spectral properties and compare them to the previous line profiles. Based on measurements of the radial velocities of the C III/N III emission lines near 4640 Å and the C IV absorption lines near 5800 Å, we infer that HD 148937 is likely a high-mass, double-lined spectroscopic binary. Combining the spectroscopic orbit with an archival interferometric measurement of the apparent separation of the equal brightness components, we tentatively conclude that HD 148937 consists of two O-type stars with masses of approximately 34 and 49 $M_{\odot}$, orbiting in an eccentric ($e = 0.75$), long-period ($P_{\rm orb} \sim 26$ yr) orbit. We discuss the potential relationship of the binary system to the peculiar properties of HD 148937, and propose future observations to refine the orbital and stellar properties.

Key words: binaries: spectroscopic – stars: massive – stars: rotation.

1 INTRODUCTION

Magnetism in O-type stars is a recently discovered phenomenon: the first magnetic O-type star was reported only in 2002 (Donati et al. 2002), and since that time large-scale surveys such as the CFHT's MiMeS (Wade et al. 2016; Grunhut et al. 2017) and ESO's BOB (Morel et al. 2015) Large Programs have succeeded in identifying only a dozen in our Galaxy. As a consequence of the small sample size, our understanding of their properties is limited. The known population (e.g. Wade & MiMeS Collaboration 2015) ranges in spectral type from around O6 to O9.5. Although spectral types are variable and luminosity classes challenging to establish for many magnetic O stars, most appear to be main-sequence objects. The detected magnetic fields are generally oblique dipoles, with polar strengths ranging from ∼0.1 to over 20 kG. Their magnetic fields channel their powerful winds, resulting in dense circumstellar mag-

★ E-mail: Gregg.Wade@rmc.ca
† Deceased 2018 February 22.

netospheres confined to co-rotate with the star (Petit et al. 2013). As a consequence, magnetic O stars exhibit strong variability across the electromagnetic spectrum, with line and continuum emission modulated periodically according to the stellar rotation period.

Notwithstanding their relative rarity (Grunhut et al. 2017 reported that just 7 ± 3 per cent of O stars observed in the MiMeS survey host detectable magnetic fields), recent work has shown that magnetic O stars may provide new keys to resolving a number of important, outstanding puzzles in stellar evolution, including the large component masses of some merging black holes in binary systems (Petit et al. 2017), and the occurrence of pair-instability supernovae in high-metallicity environments (Georgy et al. 2017).

HD 148937 was classified as a member of the peculiar Of?p spectral class by Walborn (1972, 1973). The spectral peculiarities that are diagnostic of this class are now known to be intimately associated with magnetism, and magnetic fields have been detected in all known Galactic members (Grunhut et al. 2017). Nazé et al. (2008, 2010) reported variability of optical spectral lines of HD 148937 with a period of 7.03 d, which they speculated may be related to the presence of a magnetic field, with the star viewed near the rotational pole.

At the time of its identification as a magnetic star in 2011 (Hubrig et al. 2011; Wade et al. 2012), HD 148937 was only the fifth known magnetic O star. It remains both the hottest and most massive star of this class ($T_{\rm eff} = 41$ kK, $M \sim 60$ M$_\odot$; Nazé et al. 2008; Wade et al. 2012, but see further discussion in Section 5 of this paper). ESPaDOnS (e.g. Silvester et al. 2012) Stokes I and V observations carried out by the MiMeS collaboration (Wade et al. 2012) detected a weak (∼300 G) longitudinal magnetic field and confirmed relatively subtle variability of both the longitudinal field and many optical spectral lines according to the 7.03 d period. Wade et al. (2012) interpreted the results in the context of the oblique rotator model (ORM; Stibbs 1950), inferring that the star hosts an oblique, dipolar magnetic field that confines the star's outflowing wind into a co-rotating dynamical magnetosphere with a magnetic wind confinement parameter (which measures the degree to which the stellar wind dynamics are influenced by the magnetic field) equal to $\eta_* = 20$. As a consequence, the periodic variability observed in the spectroscopic record is interpreted as rotational modulation according to its 7.03 d rotation period.

Many spectral lines of HD 148937 – including lines in strong emission as well as those in absorption – exhibit detectable variability according to this period (Nazé et al. 2010; see fig. 5 of Wade et al. 2012). The measured equivalent widths (EWs) of the spectral lines vary approximately sinusoidally, and emission and absorption lines vary approximately in phase. This variability is also explained by the ORM, in which rotation of the star and its oblique magnetosphere results in periodic modulation of the spectrum. For HD 148937, Wade et al. (2012) inferred a rotation axis inclination of $i \leq 30^\circ$, a magnetic obliquity $\beta \sim 40^\circ$, and a magnetic dipole strength of $B_{\rm d}$ of 1 kG.

Early studies left a number of peculiar characteristics of this system unexplained. In particular, Wade et al. (2012) commented that the star exhibits large cycle-to-cycle changes in the line profiles that probe the magnetosphere. They attributed these variations to 'intrinsic changes in the amount or distribution of emitting material with time, i.e. evolution of the magnetosphere of HD 148937'. However, they were unable to determine if the proposed evolution was secular or stochastic. They also noted that while the Zeeman signatures of HD 148937 observed in mean (least-squares deconvolved, or LSD) line profiles were very weak, a large Stokes V signal was observed in the absorption component of the He I λ5876 line. Since this line is not a particularly sensitive magnetic diagnostic, the appearance of a strong Zeeman signature in this line (while being absent from other lines of comparable magnetic sensitivity) was not straightforwardly understood by Wade et al. (2012).

Finally, HD 148937 is distinguished from other magnetic O stars by its remarkable bipolar nebula, NGC 6164/5 (see Mahy et al. 2017, and references therein). Recently, Mahy et al. (2017) analysed Spitzer and Herschel observations of the NGC 6164/5 nebula to constrain its global morphology, kinematics and abundances, and the evolutionary status of the central star. They concluded that the structure of the nebula is particularly complex and is composed of a close bipolar ejecta nebula, an ellipsoidal wind-blown shell, and a spherically symmetric Strömgren sphere. The combined analyses of the known kinematics and of the new abundances of the nebula suggest either a helical morphology for the nebula, possibly linked to the magnetic geometry, or the occurrence of a binary merger. The latter hypothesis would be of great interest since binary mergers have been proposed as a potential pathway to the generation of magnetic fields in massive stars (e.g. Langer 2012) .

HD 148937 was resolved as an interferometric binary in the course of the southern massive stars at high angular resolution survey (SMASH + ; Sana et al. 2014). Those authors reported that HD 148937 is an equal brightness stellar pair ($\Delta m = 0.00 \pm 0.02$ in H band) with separation $\rho = 21.05 \pm 0.67$ mas. Sana et al. (2014) further detected a faint ($\Delta H = 5.39 \pm 0.15$) companion at 3.30 ± 0.06 arcsec. Interestingly, none of the previous spectroscopic and imaging studies of the system (Nazé et al. 2008, 2010; Wade et al. 2012; Mahy et al. 2017) have reported any direct evidence of binarity.

The measured angular separation can be leveraged to determine the instantaneous projected physical separation of the equal brightness pair. The revised Hipparcos parallax implies a distance $d = 0.43 \pm 0.11$ kpc, yielding a separation of 8.9 au.[1] On the other hand, the Gaia DR2 parallax (Lindegren et al. 2018) yields a significantly greater distance of 1.14 ± 0.06 kpc, which implies an instantaneous separation nearly three times larger. However, both results may be compromised by the binarity (see Section 6.1).

In this paper, we report a significant, unprecedented change in the optical line profiles of HD 148937 that stands in stark contrast to the historical record of its periodic variability. Potential origins of the unexpected variability could be associated with the probable binarity detected by interferometry. A companion of comparable mass and luminosity to the magnetic star might, for example, also be detectable spectroscopically, and its orbital motion might translate into spectral variability. Alternatively, the two stars might interact episodically or periodically, or one of the components might undergo instability and eruption, e.g. a luminous blue variable (LBV)-like eruption. Another more exotic possibility is a significant reconfiguration of the stellar magnetosphere.

In order to better understand the origin of the change of the spectrum of HD 148937, we describe and analyse new spectroscopic observations that, in combination with archival data, provide new insight into the character of the HD 148937 system.

[1] We note that the paper by Sana et al. (2014) appears to contain a typo since those authors report an instantaneous projected separation of 40 au based on the Hipparcos distance. We note furthermore that the article reports two slightly different values of ρ. H. Sana (private communication) confirms that $\rho = 21.05 \pm 0.67$ mas as reported in table 1 of that paper is in fact the correct value.

2 OBSERVATIONS

2.1 Optical spectroscopy

High-resolution, high signal-to-noise ratio (S/N) spectra of HD 148937 were obtained in 2015 August, 2016 September, 2017 April, 2017 May, and 2017 June in the context of the ESO Diffuse Interstellar Band Large Exploration Survey (EDIBLES) Large Program (Cox et al. 2017).

HD 148937 was observed with the UVES spectrograph (Dekker et al. 2000) mounted on the Very Large Telescope at the Paranal Observatory. UVES covers the optical spectrum from 305 to 1042 nm at high spectral resolving power ($R \sim 71\,000$ in the near-UV/blue to $R \sim 107\,000$ in the red part of the spectrum). The scientific goals of the EDIBLES program require a very high S/N for each of the target spectra; typically the S/N is 700–1000 depending on the wavelength range. To achieve this data quality, additional calibration files and data reduction steps are necessary (see Cox et al. 2017 for details). HD 148937 was observed in total on five different occasions by EDIBLES; however, on each visit only part of the spectrum was observed.

Additional spectroscopic observations of HD 148937 were obtained during the intensive high-resolution spectroscopic campaign of Southern Galactic O- and WN-type stars (the 'OWN Survey'; Barbá et al. 2010, 2017). The data were obtained using the REOSC Cassegrain spectrograph[2] in cross-dispersed mode attached to the 'Jorge Sahade' 2.15 m telescope at the Complejo Astronómico El Leoncito (CASLEO, Argentina; $R = 15\,000$, $3600 \leq \lambda \leq 6100$ Å) and the échelle spectrograph at the 2.5 m du Pont telescope of Las Campanas Observatory (LCO), in Chile ($R = 40\,000$, $3450 \leq \lambda \leq 9850$ Å). Observations were collected between 2006 May and 2017 August. For wavelength calibration of CASLEO and LCO spectroscopic observations, we obtained calibration lamp (Th-Ar) exposures immediately before or after each target integration, at the same telescope position. The spectra were processed and calibrated using standard IRAF[3] routines.

One spectrum was obtained with the Magellan Inamori Kyocera double Echelle spectrograph, MIKE (Bernstein et al. 2003) on the 6.5m Magellan II (Clay) telescope. HD 148937 was observed through a 0.7 arcsec slit yielding $R \sim 40\,000$ in the blue side (3350–5000 Å) and $R \sim 33\,000$ in the red side (4900–9500 Å). Both detectors were read out in 2×2 binning mode. The S/N is around 200 in the region containing He I λ5876. The data were reduced with IRAF echelle routines.

A total of 10 FEROS spectra, five of which were first discussed and measured by Nazé et al. (2008), were also included. We also include a single spectrum obtained using the UCLES spectrograph at the Anglo-Australian Telescope in 1995, that was also discussed and analysed by those authors.

Finally, we also included a single UVES–POP observation (Bagnulo et al. 2003) obtained in 2002, and a subset of the ESPaDOnS spectra (obtained in 2009 and 2010) reported by Wade et al. (2012).

We note that while some other spectra of HD 148937 may exist in the archives, these data either do not add significantly (typically having been acquired at dates similar to the data in hand) or are lacking coverage of the key spectral features (i.e. the λλ5800 and 4640 features) used in our study.

All of the spectra used in this study are summarized in Table 1.

Table 1. Visible spectroscopy of HD 148937 employed in this investigation and measurements of the heliocentric radial velocities of the N III/C III emission line complex at ∼4640 Å and the C IV absorption lines at 5801/11 Å. The single UCLES observation (marked with a ∗), first reduced and analysed by Nazé et al. (2008), has been re-reduced and re-measured for this study.

HJD −2400 000	UT date	Instrument	RV λ4640 (km s^{-1})	RV λ5800 (km s^{-1})
49 822.5	1995-04-15	UCLES∗	− 24.3 ± 1	− 23.9 ± 3
52 332.841	2002-02-27	UVES	− 15.5 ± 1	–
52 783.757	2003-05-24	FEROS	− 17.6 ± 1	− 22.5 ± 3
52 784.749	2003-05-25	FEROS	− 17.8 ± 1	− 21.4 ± 3
53 131.618	2004-05-06	FEROS	− 18.3 ± 1	− 25.0 ± 3
53 509.728	2005-05-19	FEROS	− 17.6 ± 1	− 23.8 ± 3
53 547.535	2005-06-26	FEROS	− 17.4 ± 1	− 28.2 ± 3
53 866.8	2006-05-11	CASLEO	− 12.4 ± 3	− 24.2 ± 4
53 871.828	2006-05-16	CASLEO	− 14.0 ± 3	− 32.3 ± 5
53 874.758	2006-05-19	du Pont echelle	− 19.6 ± 1	− 27.9 ± 3
53 898.789	2006-06-12	FEROS	− 17.4 ± 1	− 20.9 ± 3
53 951.543	2006-08-04	FEROS	− 17 ± 1	− 23.3 ± 3
53 920.672	2006-07-04	du Pont echelle	− 16.9 ± 1	− 30.4 ± 3
53 938.632	2006-07-22	du Pont echelle	− 18.4 ± 1	− 31.9 ± 3
53 955.53	2006-08-08	MIKE	− 18.6 ± 1	− 32.3 ± 3
54 210.82	2007-04-20	FEROS	− 18.3 ± 3	− 33.8 ± 4
54 220.798	2007-04-30	CASLEO	− 10.2 ± 3	− 28.1 ± 4
54 252.711	2007-06-01	CASLEO	− 4.6 ± 3	− 29.4 ± 4
54 286.644	2007-07-05	CASLEO	− 8.0 ± 3	− 33.7 ± 4
54 511.873	2008-02-15	CASLEO	− 11.1 ± 3	− 35.7 ± 4
54 582.734	2008-04-26	CASLEO	− 16.3 ± 3	− 30.1 ± 4
54 608.737	2008-05-22	CASLEO	− 13.3 ± 3	− 38.4 ± 4
54 642.735	2008-06-25	CASLEO	− 17.4 ± 3	− 28.1 ± 4
54 659.564	2008-07-12	CASLEO	− 17.6 ± 3	− 34.3 ± 4
54 904.882	2009-03-14	FEROS	− 17.8 ± 2	− 25.8 ± 3
54 914.909	2009-03-24	FEROS	− 18.5 ± 2	− 23.5 ± 3
54 955.047	2009-05-03	ESPaDOnS	− 17.2 ± 1	− 24.3 ± 3
55 078.728	2009-09-04	ESPaDOnS	− 18.9 ± 1	− 22.7 ± 3
55 342.751	2010-05-26	du Pont echelle	− 17.5 ± 1	− 32.0 ± 3
55 400.771	2010-07-23	ESPaDOnS	− 17.6 ± 1	− 25.3 ± 2
55 403.778	2010-07-26	ESPaDOnS	− 16.1 ± 1	− 23.7 ± 2
56 436.738	2013-05-24	du Pont echelle	− 26.1 ± 1	− 22.8 ± 3
56 813.69	2014-06-05	du Pont echelle	− 50.9 ± 2	− 6.3 ± 3
57 251.589	2015-08-17	UVES	− 55.1 ± 1	− 0.8 ± 2
57 644.548	2016-09-13	UVES	− 39.1 ± 1	
57 867.755	2017-04-24	UVES	− 34.0 ± 1	− 18.5 ± 2
57 890.906	2017-05-17	UVES	− 35.9 ± 1	
57 924.5	2017-06-20	UVES	− 34.0 ± 1	
57 933.636	2017-06-29	du Pont echelle	− 31.6 ± 1	− 15.1 ± 3
57 934.654	2017-06-30	du Pont echelle	− 31.3 ± 1	− 17.7 ± 3
57 935.654	2017-07-01	du Pont echelle	− 31.1 ± 1	− 17.1 ± 3
57 936.666	2017-07-02	du Pont echelle	− 31.8 ± 1	− 16.2 ± 3
57 980.614	2017-08-15	du Pont echelle	− 31.7 ± 1	− 13.1 ± 3
57 981.621	2017-08-16	du Pont echelle	− 32.6 ± 1	− 15.1 ± 3
57 983.574	2017-08-18	du Pont echelle	− 31.8 ± 1	− 15.2 ± 3

2.2 X-ray flux

New X-ray observations were acquired to investigate if the X-ray emission of HD 148937 has been impacted by the phenomena responsible for the recent spectroscopic changes (as is further discussed in Section 6.3).

[2]On long-term loan from the University of Liège.

[3]IRAF is distributed by the National Optical Astronomy Observatories, which are operated by the Association of Universities for Research in Astronomy, Inc., under cooperative agreement with the National Science Foundation.

We obtained a new observation of HD 148937 with *Chandra* (Weisskopf, O'dell & van Speybroeck 1996; ObsID = 20148, 9ks duration) in 2018 June. The source spectrum was extracted using 'specextract' under CIAO v4.9 in a circle centred on the SIMBAD coordinates of HD 148937 and with 5 pixels radius. The background spectrum was extracted in the surrounding annulus with external radius of 15 pixels. Response matrices necessary for flux and energy calibration were calculated after extraction, and the spectrum was grouped to reach a minimum of 15 counts per bin. To avoid pile up, the data were obtained only for a subarray of ACIS (chip #7) in TE (timed exposure) mode and using a frame time of 0.4 s.

As appropriate for massive stars, the spectral fitting was done within Xspec using an absorbed optically thin thermal emission model of the type *wabs* × *phabs* × (*apec*$_1$ + *apec*$_2$), considering plasma abundances fixed to those of Anders & Grevesse (1989). The first component (*wabs*) represents the interstellar absorption, which was fixed to the appropriate value (i.e. absorbing column $N_{\rm H}^{\rm int} = 4 \times 10^{21}$ cm^{-2}, see Nazé, Zhekov & Walborn 2012b and references therein). The second one (*phabs*, which has a single fitted parameter $N_{\rm H}^{\rm add}$) accounts for potential circumstellar absorption. The last components (*apec*$_{1,2}$) represent the thermal emission by the hot plasma. Two components are needed to fit well the observed spectra (see Naze et al. 2012b); each one has two free parameters: the temperature (*kT*) and the normalization factor (*norm*) that is linked to the emission measure of the plasma. As in Nazé et al. (2012b), there are two solutions of similar quality ($\chi^2 \sim 1$): the 'cool' solution has $N_{\rm H}^{\rm add} = (0.34 \pm 0.08) \times 10^{22}$ cm^{-2}, $kT_1 = 0.29 \pm 0.03$ keV, $norm_1 = (1.1 \pm 0.4) \times 10^{-2}$ cm^{-5}, $kT_2 = 2.02 \pm 0.09$ keV, and $norm_2 = (3.20 \pm 0.15) \times 10^{-3}$ cm^{-5}; the 'hot' one has $N_{\rm H}^{\rm add} = (0.07 \pm 0.08) \times 10^{22}$ cm^{-2}, $kT_1 = 0.74 \pm 0.03$ keV, $norm_1 = (2.0 \pm 0.4) \times 10^{-3}$cm^{-5}, $kT_2 = 2.6 \pm 0.2$ keV, and $norm_2 = (2.25 \pm 0.17) \times 10^{-3}$ cm^{-5}. The observed flux in the 0.5–10.keV energy range is $(3.3 \pm 0.1) \times 10^{-12}$ erg cm^{-2} s^{-1}.

3 LONG-TERM LINE PROFILE VARIABILITY OF HD 148937

The change in the character of the spectrum of HD 148937 was first identified by the EDIBLES team from profiles of the He I λ5876 line obtained in 2015 (on JD 2457251, which we will refer to as 'the 2015 spectrum'). As illustrated in the left-hand panel of Fig. 1, the profile of the λ5876 line maintained the same essential quasi-P Cyg morphology in observations obtained from 1995 to 2010. The (small) range of variability of the profiles acquired during this period is in good general agreement with the 7.03 d rotational variability measured in past studies.

As shown in the right-hand panel of Fig. 1, the 2015 UVES spectrum revealed a stark change in the λ5876 profile; the initiation of this change can be traced back to at least 2013, and the profiles appear to be returning to normal in 2017 (see Fig. 1 and next). Our principal aim in this paper is to understand this phenomenon via a deeper examination of the spectroscopy.

In Fig. 2, we illustrate the profiles of selected spectral lines in the 2015 spectrum, shown in red. As the 2015 observation included only the '346' (3042–3872 Å) and the '564' (4616–6653 Å) settings of UVES, we employ the 2016 UVES observation (JD 2457644, obtained in the '437' setting, yielding wavelength coverage from 3752–4988 Å) for the He II λ4686 line, which was located at the edge of an order in the 2015 spectrum. These data are shown in green. For comparison, we also show the 2017 April UVES spectrum (JD 2457867) for all lines (except H α because this line was saturated) and the two ESPaDOnS spectra (Wade et al. 2012) selected to characterize the full range of short-term (rotational) variability of the spectrum observed in 2009/10. These are shown in black.

A significant change of both line position and shape is observed in essentially all lines in 2015–16, including both emission and absorption lines. In particular, we note that emission lines sensitive to the magnetosphere (i.e. those observed by Nazé et al. 2008 and Wade et al. 2012 to vary significantly according to the 7.03 d rotational period: Balmer lines, He I λ5876, He II λ4686), emission lines insensitive to the magnetosphere (exhibiting weak to no detectable 7.03 d variability: the λ4640 complex of C III and N III lines, He I λ4921), and photospheric absorption lines (N IV λ5200/04, He II λ5411, C IV λ5801/11) show significantly different morphologies in the 2015–16 spectra relative to the historical record as illustrated by the ESPaDOnS spectra. Moreover, the 2017 spectra show profiles that are generally more similar to those observed historically, supporting our impression that 2015 represented the extreme of the event, after which the spectrum has been gradually returning to normal.

In the remainder of this report, we focus our attention on one notable feature of the variability of HD 148937: the apparent wholesale shifts of the C III and N III λ4630 − 50 emission peaks, and the λ5801/11 absorption cores, in the profiles illustrated in Fig. 2. We note in particular the fact that the absorption lines appear to shift in the direction opposite to that of the emission lines.

4 RADIAL VELOCITIES OF THE C III/N III λ4634 − 47 EMISSION LINES AND THE C IV λ5801/11 ABSORPTION LINES

We have determined the radial velocities (RVs) of the N III λλ4634.140, 4640.640 and C III λ4647.418 lines by measuring the wavelengths of the sharp peaks of the emission of these three lines in each spectrum. Due to blending, we did not measure the C III λ4650 line RV. We computed the simple mean RV of the emission lines. These values are reported in the fourth column of Table 1. Similarly, we determined the RVs of the C IV λλ5801.310, 5811.970 lines by measuring the wavelengths of the absorption cores of these two lines. Again, we computed the simple mean RV of these absorption lines. These values are reported in the fifth column of Table 1. Note that some spectra did not cover one or the other of these regions, explaining blank entries in Table 1.

Conti, Garmany & Hutchings (1977) reported RVs of a number of lines in the spectrum of HD 148937 with typical uncertainties of order 5 km s^{-1}. While line-to-line velocity differences were reported, no significant velocity variations were reported by those authors, nor did they report RVs for the λλ4640 or 5800 lines. Similar results were reported by Nazé et al. (2008).

We re-measured the RVs of the UCLES spectrum and FEROS spectra discussed by Nazé et al. (2008), finding velocities in reasonable agreement with the values reported in those papers.

Finally, we also considered the SMARTS RVs discussed by Nazé et al. (2008). However, since these measurements are of lower precision, they did not add significantly to our analysis. Therefore, we will not discuss them any further here.

We checked for systematic errors in the RVs by verifying the absence of any detectable shifts of the strong, sharp Na I interstellar features located close to the C IV absorption lines. Random uncertainties were estimated for each line from the dispersion of measurements from independent spectra obtained close in time (when available), or from multiple measurements of individual spectra (when they were not). These values, typically ∼1−2 km s^{-1} for the

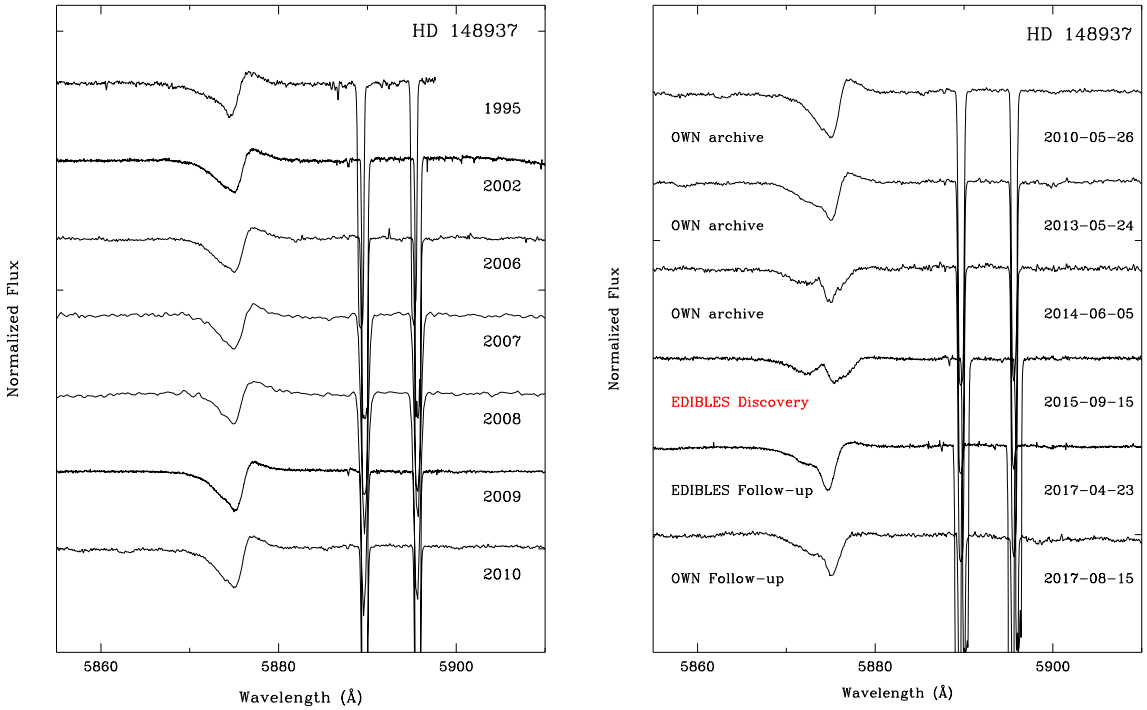

Figure 1. *Left* – Illustration of the telluric-corrected line profiles of He I λ5876 of HD 148937 prior to 2011. All profiles except the 1995 (UCLES) observation are qualitatively consistent with the range of profile shapes attributed to rotational modulation by Wade et al. (2012). The UCLES profile shows a weaker extended blue wing that distinguishes it, and which may indicate that another episode, similar to that inferred to be occurring now, was underway at that time. *Right* – Illustration of the change in the character of the He I λ5876 profile in 2013 and its subsequent evolution.

λ4640 emission lines and ∼2−4 km s^{-1} for the λ5800 absorption lines, are reported in Table 1.

Both the λλ4640 and 5800 RVs exhibit significant changes between 1995 and 2017. These changes are much larger than the ∼2 km s^{-1} scatter of the RVs of these lines measured from the full collection of ESPaDOnS spectra of Wade et al. (2012). We note in particular that (i) in accordance with our initial impression, the λλ4640 and 5800 RVs vary in opposition to one another, and (ii) the largest difference in RV between the λλ4640 and 5800 lines (approximately 54 km s^{-1}) occurred in 2015, at the time of the largest distortion of the He I λ5876 line.

5 HD 148937 APPEARS TO BE A MASSIVE SB2

The character of the RV measurements is highly suggestive of binary motion, in which the λ4640 emission lines diagnose the RV of one stellar component, and the λ5800 absorption lines diagnose the other component. To test this hypothesis, we employed the IDL orbital fitting code XORBIT (Tokovinin 1992) to model the orbit. This code determines the best-fitting orbital period $P_{\rm orb}$, Julian date of periastron passage (T), eccentricity (e), longitude of the periastron (ω), semi-amplitudes of each component's RVs (K_1 and K_2), and the RVs of the centre of mass ($\gamma_{1,2}$ for both components), performing least-squares fits to the measured RVs.

An acceptable fit to the data is achieved with the orbital hypothesis. The spectroscopic data appear to cover only slightly more than one orbital period, and with only sparse sampling of the phase of periastron passage. As a consequence, the RVs allow two distinct periods to fit the data more or less equally well. As illustrated in Fig. 3, the residuals from the best-fitting orbital solutions for a range of fixed period (from 2000 to 20 000 d at 20 d steps) confirm that there are reasonable solutions for periods around 6500 d (formally 6617 ± 50 d) and $\gtrsim$ 9000 d (with a formal best fit at 9591 ± 350 d), with this longer period actually giving marginally better residuals. The ambiguity in P arises essentially because we are as yet unable to determine if the first (UCLES) observation falls before or after the previous periastron passage. Nevertheless, the two periods yield similar orbital geometries, with roughly the same RV amplitude ratios and zero points. The eccentricity derived for the longer period is somewhat higher (0.75 versus 0.58). While periods larger than 9000 d are relatively unconstrained by the existing data, we note that the implied projected mass of the primary star becomes rapidly unphysical for periods longer than 10 000–11 000 d. This is also illustrated in Fig. 3.

Nota et al. (1996) reported acquiring an ESO EMMI spectrum of HD 148937 between 1991 September 17and 20. While the original data no longer appear to be available, illustrations of line profiles provided in their paper suggest that the λ5876 line was likely experiencing distortions at that time similar to those exhibited in 2015/2017. In particular, the λ5876 profile illustrated in their paper bears a strong similarity to those obtained in 2013 May and 2017 April/August (see Fig. 1). These observations bracket the epoch of strongest distortion of the line. Since the observation obtained by Nota et al. (1996) was obtained roughly 8500 d prior to the most recent periastron passage, if we suppose that the spectroscopic variability is associated with orbital phase (noting that the appearance of line-profile anomalies in 2014/15 coincided closely with periastron passage, regardless of the adopted orbital period) this would a imply period of ∼8000 d (if the EMMI spectrum was obtained before the previous periastron passage) or ∼9500 (if it was obtained after the previous periastron passage). The latter time-scale is consistent with the long-period model, which we tentatively adopt as our reference model.

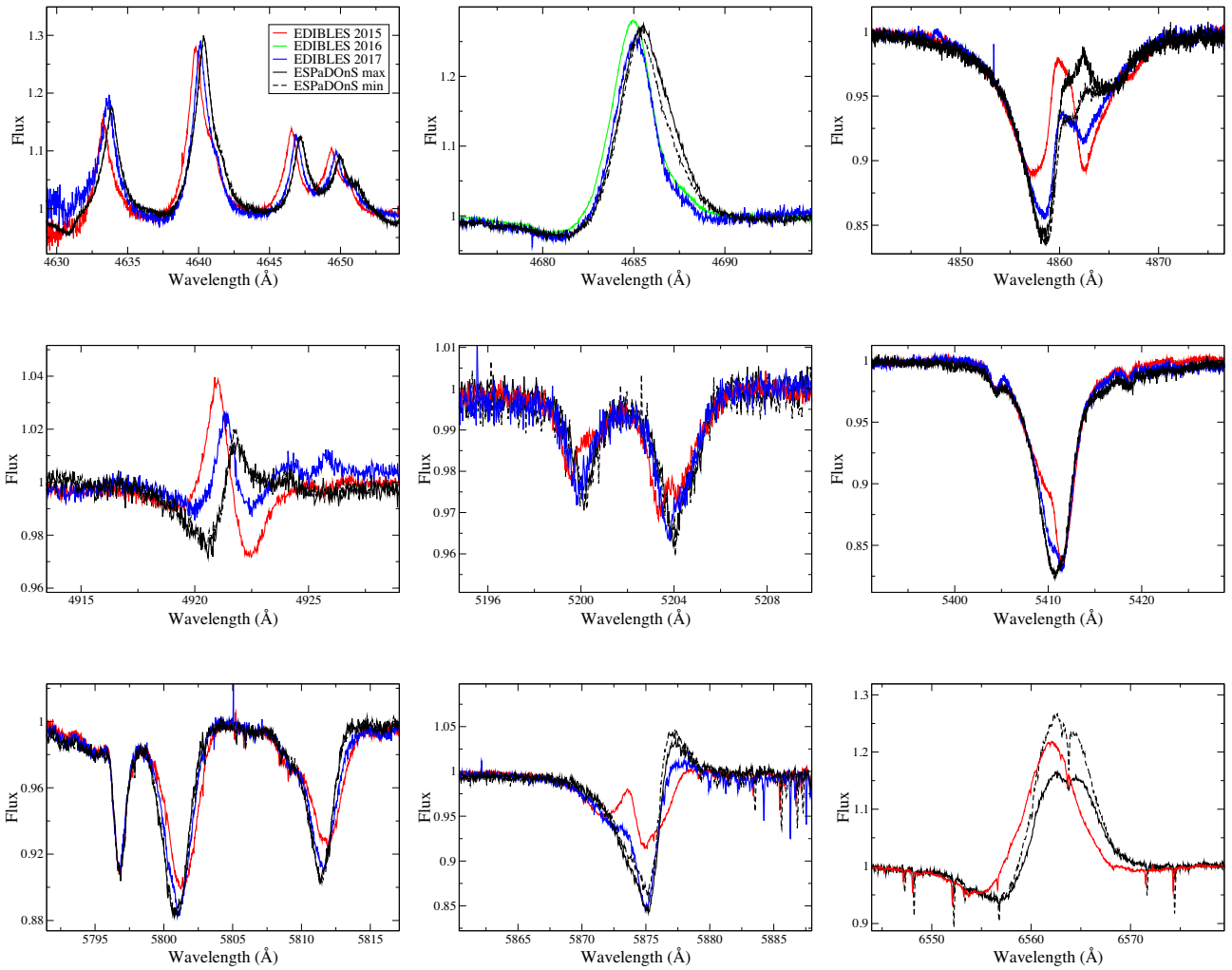

Figure 2. The black (solid and dashed) profiles show the range of variability of each spectral line in the ESPaDOnS data set of Wade et al. (2012). The red, green, and blue profiles show the EDIBLES observations obtained in 2015 (JD 2457251), 2016 (JD 2457644), and 2017 (JD 2457867), respectively. Spectra are in the heliocentric reference frame and have not been corrected for telluric absorption.

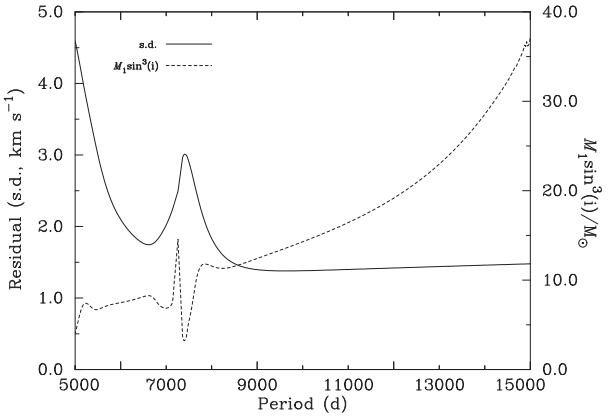

Figure 3. *Solid curve* – Residuals from best-fitting orbital solutions for a range of fixed period. *Dashed curve* – Implied projected mass of the primary star versus period.

Using XORBIT, we were able to achieve a reasonable simultaneous fit to the measured RVs of both sets of lines, for both orbital periods described above. Fig. 4 illustrates the RVs of both stars versus JD and phased assuming the longer period. The RV semi-amplitudes imply a mass ratio $M_1/M_2 = 1.5$, with an uncertainty of 15–20 per cent. The orbital parameters derived from the SB2 solution adopting the longer and shorter periods are summarized in Table 2. Given the limited quality and coverage of the data, we focus on the general characteristics of the solution rather than the details.

6 DISCUSSION

We have reported a remarkable change of the spectrum of the magnetic Of?p star HD 148937 that departs qualitatively from the long historical record of the star's periodic 7.03 d variability.

Our measurements of the λλ4640 (the N III λλ4634, 4640 and C III λ4647 emission lines) and 5800 (the λλ5801, 5811 absorption lines) RVs show convincingly that the spectrum variation is significantly influenced by binary motion of two stellar components. If our orbital interpretation is correct, then it appears that the λ4640

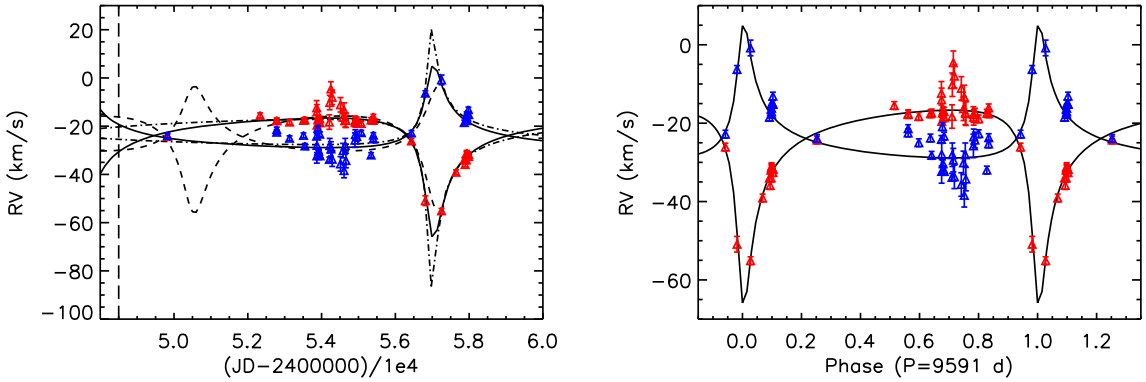

Figure 4. Model orbits fit to the RVs. *Left* – RV showing models versus JD corresponding to $P = 9591$ d (the 'long-period solution', solid curve), $P = 6617$ d (the 'short-period solution', dashed curve), and an arbitrary model with $P = 13000$ d (a 'very long period' solution, dot–dashed curve). *Right* – RVs phased and folded according to the $P = 9591$ d period. In both plots, the blue symbols are the λ5800 measurements, corresponding to the primary component. The red symbols are the λ4640 measurements, corresponding to the secondary star. The vertical dashed line in the left-hand panel represents the date of the EMMI observation by Nota et al.

Table 2. Orbital solution computed from the λλ4640 and 5800 RVs.

Quantity	Long period solution	Short period solution
P (d)	9591 ± 350	6617 ± 50
T (d)	2456991 ± 20	2457116 ± 35
K_1 (km s^{-1})	17.3 ± 2.0	13.5 ± 1
K_2 (km s^{-1})	25.2 ± 2.5	20.1 ± 0.5
γ_1 (km s^{-1})	−22.4 ± 0.5	−21.6 ± 0.5
γ_2 (km s^{-1-1})	−24.1 ± 0.2	−24.9 ± 0.2
e	0.75 ± 0.03	0.58 ± 0.02
ω (°)	342 ± 2	347 ± 3
M_1/M_2	1.5 ± 0.3	1.5 ± 0.2
$M_1 \sin^3 i$ ($M_\odot$)	13.1 ± 5	8.5 ± 1
$M_2 \sin^3 i$ ($M_\odot$)	9.0 ± 4	5.7 ± 1
$a \sin i$ (au)	24.8 ± 3.5	16.6 ± 0.8

RVs are principally sensitive to the motion of one star (the lower mass secondary), while the λ5800 RVs trace the motion of the higher mass primary star. Examination of the variations of the H α and He II λ4686 profiles shown in Fig. 2 – lines observed by Nazé et al. (2008); Wade et al. (2012) to vary strongly according to the 7.03 d period – reveals that they also show bulk RV shifts qualitatively consistent with the λ4640 lines. Since we expect that these emission lines arise principally in the magnetosphere, we tentatively interpret this to imply that the lower mass secondary star is also the magnetic star.

6.1 Astrometric considerations

As noted in Section 1, long baseline interferometric observations of HD 148937 obtained with VLTI/PIONIER by Sana et al. (2014) revealed two equally bright components in the H band ($\Delta H = 0.00 \pm 0.02$). Those authors assumed the Hipparcos distance to derive the instantaneous projected separation. However, the Hipparcos parallax they used is only significant at 3σ confidence. Given $V = 6.7$ and $E(B - V) = 0.61$ (Mahy et al. 2017), adopting the Hipparcos distance the implied absolute magnitude of the system is $M_V = -3.3$, which is somewhat faint for an O star (and another 0.75 mag fainter if we correct for a roughly equal brightness companion).

As discussed in the introduction, the recent Gaia DR2 parallax re-evaluation (Lindegren et al. 2018) implies a distance of 1.14 ± 0.06 kpc. However, Lindegren et al. (2018) explicitly discuss DR2 results for unresolved/partially resolved multiple systems. In particular, they note: 'In this release, all sources beyond the solar system are still treated as single stars, that is, as point objects whose motions can be described by the basic five-parameter model. For unresolved binaries (separation $\lesssim 100$ mas), the photocentre is consistently observed and the astrometric parameters thus refer to the position and motion of the photocentre in the wavelength band of the G magnitude. Orbital motion and photometric variability may bias the astrometric parameters for such sources'. Given the results of Sana et al. (2014) reporting the detection of a companion of similar H-band magnitude at a separation of about 21 mas, we interpret the DR2 results with a degree of scepticism.

Given the weak constraints from the Hipparcos parallax, and our concerns about the reliability of the Gaia parallax, it may well be more secure to adopt a distance based on assumed membership of Ara OB1 (e.g. Humphreys 1978, which lists $m - M = 10.7$, implying $d = 1.4$ kpc). We note that Mahy et al. (2017) quote a distance of 1.3 kpc, while Mel'Nik & Dambis (2009) give 1.1 and 2.8 kpc for Ara 'OB1A' and 'OB1B', respectively. Distances of order 1 kpc are more consistent with the fluxes expected of typical O stars, and also more consistent with the Gaia parallax (notwithstanding the caveat noted above). It therefore seems plausible that the distance to HD 148937 is similar to that implied by the Gaia parallax, and considerably larger than implied by the Hipparcos parallax (i.e. 1.0–1.4 kpc rather than 425 pc). This conclusion is also supported by the interstellar Ca II column density reported by Hunter et al. (2006) interpreted using the relationships of Smoker, Keenan & Fox (2015).

Gaia DR2 also reports a $G = 12.1$ (as compared to $G = 6.6$ for HD 148937) source located at an angular separation of 3.3 arcsec. This source certainly corresponds to the $\Delta H = 5.4$ neighbour observed by Sana et al. (2014). The parallax of this source yields a distance somewhat smaller than (but within 2σ of) the brighter source. However, given the caveat discussed above, it is not clear that we can draw any significant conclusions regarding its physical association with the main system. Certainly the formal parallaxes are not very different from one another.

Knowing the spectroscopic orbit, we can in principle calculate the projection of the orbit on to the plane of the sky, given two additional angles: the position angle of the ascending node and the orbital inclination (e.g. Harries & Howarth 1996). The former is of no

particular interest (it merely defines the orientation of the projected orbit), but we can readily plot the projected linear separation of the components as a function of orbital phase for any given inclination.

Fig. 5 (left-hand panel) presents such plots for the longer orbital period; the curves are for sin(i) = 1.0, 0.9, 0.8... (from the bottom up). At the moment, we only have one direct measurement of the angular separation from SMASH + ; we take $\rho = 21.05$ mas at JD 2456088. Converting the date to phase assuming the longer period, and the angular measure to linear measure, we can add this observation to the plots – shown as dots for assumed distances of 1.0, 1.2, and 1.4 kpc (bottom to top). Because the curves in these plots are not parallel, additional astrometric observations can, in principle, constrain distance and inclination separately. But even this single observation has some utility, as it constrains $\sin i$ to 0.65 ± 0.1 for this plausible range of distance.

Adopting $\sin i = 0.65 \pm 0.1$ (or $i = 40 \pm 8^{\circ}$), the implied masses of the components are 49 and 34 $M_{\odot}$ for the primary and secondary, respectively. As illustrated in Fig. 5 (right-hand panel), the full range of permitted masses – given the uncertainty on both distance and period – for the secondary is rather large. (We note that Wade et al. 2012 reported a mass of HD 148937 of 60 $M_{\odot}$ but without benefit of knowledge of the system's multiplicity.) The other known Of?p stars have masses ranging from 30 to 5 $M_{\odot}$ (e.g. Wade & MiMeS Collaboration 2015), in agreement with the result for the secondary, but consistent with the mass of either star given the uncertainties.

6.2 Spectrum formation and composition

Why do the λλ4640 and 5800 features seem to distinguish the motion of the stars so clearly? It is known that the N III λλ4634/40/42 and C III λλ4647/50/52 emissions are strongly peaked at spectral type O5 in Ofc stars (Walborn et al. 2010). This spectral type seems too early given the secondary's mass, but strong and variable C III λλ4647/50/52 emission is also a defining characteristic of the magnetic Of?p stars. Moreover, examining spectra in our possession reveals that the N III and C III emission line intensities of HD 148937 are the strongest of any of the Galactic Of?p stars, and stronger than those of HD 191612 (which has the next strongest emission in this region) by about 80 per cent. It therefore seems reasonable to assume that the magnetic secondary's emission lines dominate in the λ4640 region.

EWs of the C IV λλ5801/11 lines as a function of spectral type (Fullerton, Gies & Bolton 1996) peak at O6–O7.5 for all luminosity classes. The combination of a mid-O star (strong C IV) plus a late-O star (weak C IV) of similar continuum brightness is roughly consistent with the observed EW of the λ5801 line. Such a scenario could potentially explain the sensitivity of the C IV lines to the primary's motion. We note that this necessarily implies that the more massive primary star is hotter than the magnetic secondary star. As a consequence, the identical *H*-band magnitudes of the two stars need to be understood. Non-rotating evolutionary tracks of Ekström et al. (2012) for 35 and 50 $M_{\odot}$ stars differ by somewhat less than a factor of ∼2 (i.e. 0.3 dex) in bolometric luminosity through most of the main sequence, but knowledge of the effective temperatures of the two stars and their relative radii would be necessary to evaluate the expected *H*-band flux ratio. This puzzling characteristic of the system should be investigated further once additional constraints on the masses, radii, and temperatures of the stars have been obtained.

Given that the details of the formation of the spectrum are poorly understood, it is worth evaluating if all of the observed variability could potentially be explained by the intrinsic variability of a single star. While the evidence presented above leads us to interpret the change in the spectrum of HD 148937 as a consequence of the mutual orbital motion of two massive O-type stars is compelling, it might be argued that other phenomena, e.g. asymmetric infilling of spectral lines result in the appearance of RV variations. However, we underscore that photospheric absorption lines (high ions of C and N with weak sensitivity to the magnetosphere and circumstellar environment), emission lines that are clearly sensitive to the magnetosphere (showing strong modulation according to the 7.03 d rotational period of the magnetic star), as well as emission lines that are not modulated by the rotational period, are all impacted by this episode. Qualitatively, this seems hard to explain by, e.g. variable emission resulting from enhanced mass-loss. Moreover, careful examination of the C IV λ5801 line (in particular) shown in Fig. 2 shows that its variability does not seem to be consistent with infilling by emission; the observed RV variation represents a wholesale shift of the entire line. Similarly, the λ4640 lines experience no significant change in shape, but are rather moved (fully and in tandem) to the blue in Fig. 2. Finally, the independent interferometric observation provides clear corroborating evidence of binarity in the detection of a companion of similar magnitude. We therefore conclude that a model invoking intrinsic line profile variations of a single star to explain these diverse phenomena is far less simple, and therefore less preferable, than the adopted eccentric binary interpretation, which provides a straightforward interpretation of the data, yields physical parameters that are broadly consistent with the expected properties of the components, and is quantitatively falsifiable. As a consequence, while the detailed formation of the system's spectrum clearly deserves further investigation, we conclude that the binary origin of the apparent RV variations is currently the best interpretation of the observed variability.

6.3 X-rays

The new X-ray observations were acquired to investigate if the X-ray emission of HD 148937 has been impacted by the phenomena responsible for the recent spectroscopic changes.

To avoid cross-correlation problems, we compare the fitting results described in Section 2.2 to those derived from fits to the previous *Chandra* data sets (Nazé et al. 2012b). The spectral parameters are very similar, except for a slight increase in normalization factors (e.g. for the 'cool' solution, the first normalization remains constant but the second one is 20 per cent larger). The observed flux is consequently larger, by ∼20 per cent, and this flux difference appears significant (6σ). Compared to the flux derived from older XMM data (Nazé et al. 2008), the change is even smaller (∼5 per cent).

No large change in the X-ray flux of HD 148937 is expected in the context of magnetically confined wind shocks since the small inferred inclination angle of the star leads to the magnetosphere being viewed from a similar perspective at all phases, yielding weak rotational modulation. Hence, the 20 per cent increase in flux compared to the previous *Chandra* observations likely requires a different explanation. In massive binaries, X-rays are sometimes emitted due to a strong collision between the stellar winds. In the case of long periods, as is the case here, such collisions are adiabatic in nature, and the X-ray luminosity varies as 1/separation with absorption effects only playing a role close to the periastron passage (for a review, see Rauw & Nazé 2016). The three X-ray data sets were taken at JD = 2451966.2 (XMM, Nazé et al. 2008), 2455353.6 (*Chandra*; Nazé et al. 2012b), and 2458286.8 (new *Chandra* data), which correspond to relative separations of 1.7, 1.2, and 1.1, respectively, for the long-period solution. If colliding winds alone were responsible for the X-ray emission of HD 148937, then the largest flux would have been

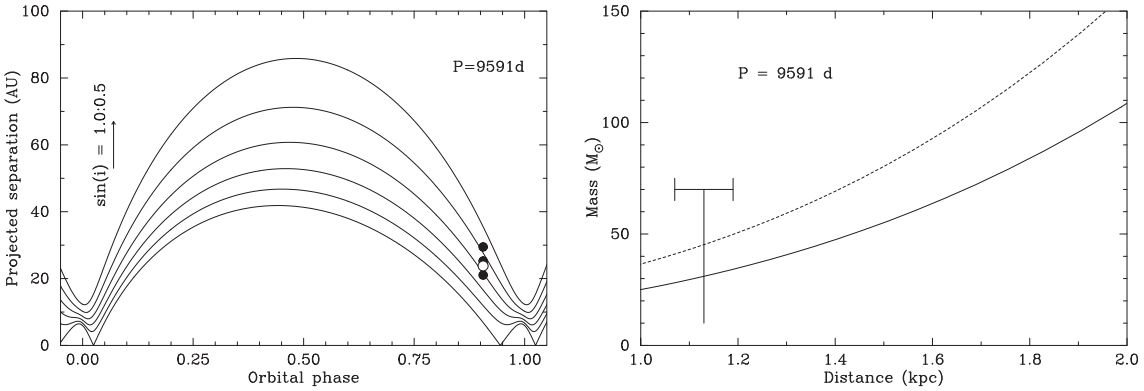

Figure 5. *Left* – Projected separation of the components of HD 148937 assuming the longer period ($P = 9591$ d) orbital solution. The curves correspond to inclinations $\sin i = 1.0$, 0.9, 0.8... (from the bottom up). The filled circles are the separation for assumed distances of 1.0, 1.2, and 1.4 kpc (bottom to top). The open circle represents the Gaia DR2 distance, for reference. *Right* – Constraint that the single SMASH + observation provides on masses as a function of distance. The two curves correspond to M_1 and M_2. The Gaia DR2 distance is indicated by the vertical line. We remind the reader that the Gaia distance may be systematically affected by the presence of the close interferometric companion.

expected for the new observation and the lowest (35 per cent lower flux) for the XMM observation, with little change between the two *Chandra* observations, but the observations indicate otherwise.

For the short-period solution, relative separations would be 1.2, 1.3, and 1.1 for the three data sets, respectively, with expected increases in flux of ∼8 and ∼15 per cent for the new data set compared to the XMM and old *Chandra* observations, respectively. At first sight, the observed X-ray properties may thus appear very compatible with the short-period scenario. However, the good agreement in amplitude changes must be considered in the context that the colliding wind contribution is small far from periastron (see e.g. Nazé et al. 2012a). For the first *Chandra* observation, the X-ray flux should be close to the canonical relation $\log(L_X/L_{BOL}) \sim -7$ naturally expected for massive stars, whereas $\log(L_X/L_{BOL}) \sim -6.25$ is derived from data. This suggests that the bulk of the X-ray emission does not come from colliding winds. Indeed, the emission level observed previously is fully compatible with predictions of confined winds models (Nazé et al. 2014). This implies that any colliding wind contribution will be diluted, leading to lower variability levels. Considering this fact, the X-ray variability of HD 148937 is thus not fully explained, but is likely not incompatible with a contribution from colliding winds in a binary system.

6.4 Other outstanding issues, and future observations

Spectral variability of Of?p stars is often accompanied by photometric changes (e.g. Walborn et al. 2004). However, photometry is scarce for HD 148937. Nazé et al. (2008) reviewed published analyses of photometric observations of HD 148937, summarizing evidence for long-term variability and performing an analysis of the Hipparcos and Tycho photometry. They concluded that no significant change or periodicity is present (see as well fig. 13 of Wade et al. 2012). In addition to the photometry discussed by those authors, ASAS-3 photometry of HD 148937 was obtained between 2000 and 2008. However, the star is in the saturation regime of the survey, and the measurements show clear evidence of saturation-related systematics. Another existing source of photometric measurements is the AAVSO[4] data base, with 2550 points since 1988 February reported by the Royal Astronomical Society of New Zealand

[4]https://www.aavso.org/

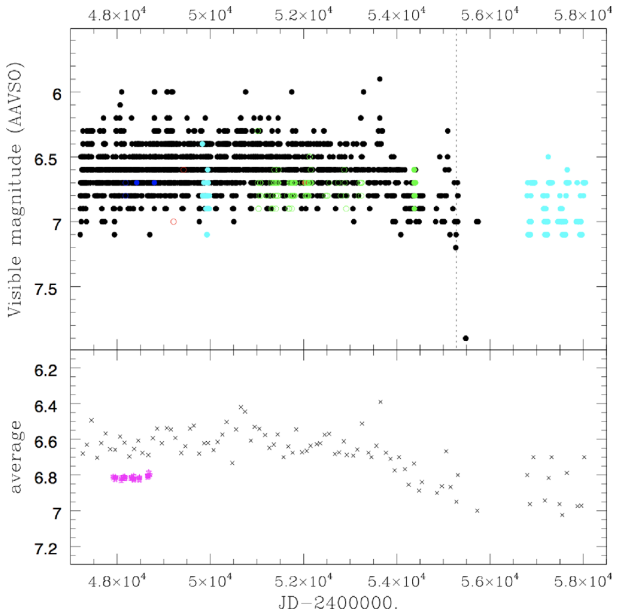

Figure 6. Visual magnitude measurements made by the RASNZ, with different observers coded by different symbols. The vertical dotted line indicates when comparison stars were changed. The lower frame shows the same data binned in 100 d averages (in grey), along with the Hipparcos photometry (in purple).

(RASNZ, Fig. 6). Unfortunately, except for five points, all values are only pre-validated; in addition, there is a gap in measurements between mid-2011 and mid-2014, an epoch of great interest in the context of this paper. Nevertheless, even if scatter is quite large, there seems to be a decline in brightness, by ∼0.2 mag since the end of 2006 (JD = 2454 000). The data were obtained by eight different observers: a single one ('JA') is responsible for 85 per cent of them, but another one ('WPX') obtained all recent ones. However, the decline is also seen in the sole 'JA' data set. Given the limited quality of the existing photometry, it is clear that little can be concluded apart from the fact that the star has exhibited no large photometric variations (i.e. greater than a few tenths of magnitudes) between 1988 and 2014. The AAVSO photometry of HD 148937

(along with the Hipparcos photometry) as a function of Julian date are illustrated in Fig. 6.

In the Introduction, we speculated that the unexpected variability may have its origin in the probable binarity reported by Sana et al. (2014). Based on our spectroscopic monitoring, we tentatively conclude that an important component of the change in the spectrum of HD 148937 is associated with variable distortion by a companion comparable in mass and luminosity to the magnetic star, in an eccentric, long-period (26 yr) orbit. For the longer period solution, the inferred semimajor axis and eccentricity imply a closest approach (around JD 2456 991, the beginning of 2014 December) of the two stars of about 9.7 au, equal to roughly 140 times the radius of a typical Of?p star. This would suggest that tidal interactions between the two components are unlikely, even at periastron. Nevertheless, both spectroscopy and unpublished interferometry (Sana, private communication) agree that the greatest distortion of the spectrum occurs when the stars are physically closest to one another. We also point out that the eccentricity could potentially be larger, given that the values obtained from our fits are derived from relatively few RV points somewhat removed from the exact date of periastron passage.

As pointed out by Mahy et al. (2017), HD 148937 is the only magnetic O-type star known to be surrounded by a nebula that can be attributed to mass-loss. θ^1 Ori C and NGC 1624-2 have surrounding nebulosities, but they are H II regions associated with the star-forming environments of these stars. The exact formation process of this nebula raises many questions. Mahy et al. (2017) suggest that multiple epochs of nebular ejection have occurred, 1.2−1.3 Myr ago, and a more recent event 0.6 Myr ago. They estimate the mass of the ionized gas in the nebula to be $\sim$12.4 $M_\odot$, but this estimate is uncertain. They discuss evolutionary scenarios in detail, but only from the perspective of a single star: a giant eruption (an LBV-like event?) triggered by the stellar wind and the magnetic field, or a merger event between two massive stars in a binary configuration. The merger scenario focuses on explaining the magnetic field of the secondary star, but arguments against it work for both secondary and primary. Such a merger would require that one of the two existing O-type stars would have previously been two lower mass stars in a tight orbit, and then through subsequent stellar and/or dynamical evolution the stars would have merged. Given that the pre-merger masses of these stars would have been substantially smaller than that of the current secondary or primary, they should have been less evolved. So, the mechanism by which such a merger would have occurred is unclear.

Wade et al. (2012) report that, compared to other lines of similar strength and Landé factor, the He I λ5876 line exhibits an anomalously strong Stokes *V* signature. In addition, the star appears to show a Stokes *V* profile given the star's relatively weak magnetic field. The *V* profile appears to be somewhat wider than the sharper principal component of its Stokes *I* LSD profile (see fig. 7 of Wade et al. 2012). It seems plausible that both of these characteristics could be a result of the SB2 nature of the system, with the Zeeman signature contributed by one component, but the Stokes *I* profile defined by contributions of both stars. Alternatively, emission might infill the blue wing of the profile. Since these spectra were obtained before the recent episode of spectral evolution began, such emission would most likely be of magnetospheric origin.

It will be very interesting to eventually determine the orientation of the binary orbit and its relationship to the nebular geometry. This will help to clarify if the binary system governs the nebular geometry, and if/to what event the magnetic field may also contribute. We note that the derived orbital inclination is in reasonable agreement with the spectroscopic constraint that the rotational axis inclination of the magnetic star be less than about 30°. As a consequence, aligned spin and orbital axes cannot be ruled out. And it may well be that both binarity and magnetism contribute to the observed nebular characteristics, e.g. binarity as the origin, with the magnetic field sculpting the 'fig. 8' shape described by Mahy et al. (2017). Moreover, wide-field imagery of the interstellar medium and nebulosity adjacent to HD 148937 (see apod.nasa.gov/apod/ap160330.html and the analysis by Romero 2006) may be indicative of larger scale and longer time-scale interactions of the system.

Could the (likely important) contribution of the presumably non-magnetic primary star to the spectrum be related to the surprising cycle-to-cycle scatter in the 7.03 d EW curves reported by Wade et al. (2012)? If the primary star exhibits episodic mass ejections (as might be inferred from the presence of the nebula), it may be stochastically variable on shorter time-scales as well. More generally, the presence of a bright second star similar in spectral type to the magnetic star has implications for the quantitative interpretation of the stellar spectrum, and of the magnetic measurements. Another, more exotic possibility is that the variability of the magnetospheric lines really does probe intrinsic variations of the magnetospheric structure. In that case, ascribing the recent variability to a significant reconfiguration of the Of?p star's magnetosphere might be plausible. However, all of this is speculation, and more detailed investigation of the spectral contributions of the two stars – before and during the 2015 event – will help to answer these questions and understand the detailed origins of the spectral evolution.

The discovery of the likely binary nature of HD 148937 is significant, as it contributes to the ongoing discussion about the relationship of binarity to massive star magnetism (e.g. Alecian et al. 2015). Nevertheless, our binary solution is not unique, and it is subject to the limitations of incomplete phase coverage and limited data quality. Dedicated spectroscopic monitoring should be continued, with a view to eventually observing the next periastron in either 2032 December (shorter period) or 2039 February (longer period). Continued interferometry should ultimately provide an independent test of the orbital model proposed here, and ultimately combining interferometry and RVs should securely determine the orbital geometry and stellar masses. In addition, future spectroscopic or spectropolarimetric monitoring covering the 7.03 d period will test if the magnetospheric configuration (and potentially more remarkably the rotational period) of the Of?p star has changed.

Simultaneously, a detailed analysis of the spectra of the components must be performed, including a fine determination of the stellar properties. This should allow evaluation if simple shifting of two spectra in velocity is sufficient to explain the observed variation, or if intrinsic variability must be invoked. The magnetic and magnetospheric properties of the Of?p star should be re-evaluated taking into account the spectral contamination of the companion. Additionally, monitoring on the rotational time-scale could serve as an immediate check if there has been any change in magnetospheric variability.

ACKNOWLEDGEMENTS

We dedicate this work to our friend and colleague Nolan R. Walborn, who passed away during the final stages of this investigation.

We thank the anonymous referee for their careful review and thoughtful comments.

This work has used data from the European Space Agency (ESA) mission *Gaia* (https://www.cosmos.esa.int/gaia), processed by the *Gaia* Data Processing and Analysis Consortium (DPAC, https://www.cosmos.esa.int/web/gaia/dpac/consortium). Funding for the

DPAC has been provided by national institutions, in particular the institutions participating in the *Gaia* Multilateral Agreement.

GAW acknowledges Discovery Grant support from the Natural Sciences and Engineering Research Council of Canada. YN acknowledges support from the Fonds National de la Recherche Scientifique (Belgium), the Communauté Française de Belgique, and the PRODEX XMM contract. RG is Visiting Astronomer, Complejo Astronómico de la República Argentina and the National Universities of La Plata, Córdoba and San Juan. RB and JA thank the DIDULS projects PR18143 and PR16142, respectively. JC and AF acknowledge support from an NSERC Discovery Grant and a SERB Accelerator Award from Western University. UCLES data from April 1995 was provided by Simon O Toole at AAT. We exploited data from ESO programs 075.D-0369(A), 077.D-0705(A), 082.C-0446(B), 082.D-0136(A), 194.C-0833(D), 194.C-0833, 266.D-5655(A). The authors acknowledge the contribution of H. Sana, who provided helpful discussion and comments, access to unpublished interferometric results, and kind support to GAW during a research visit to KU Leuven.

REFERENCES

Alecian E. et al., 2015, in Meynet G., Georgy C., Groh J., Stee P., eds, Proc. IAU Symp. 307, New windows on massive stars: asteroseismology, interferometry, and spectropolarimetry, Cambridge University Press, Cambridge, p. 330
Anders E., Grevesse N., 1989, Geochim. Cosmochim. Acta, 53, 197
Bagnulo S., Jehin E., Ledoux C., Cabanac R., Melo C., Gilmozzi R. ESO Paranal Science Operations Team, 2003, The Messenger, 114, 10
Barbá R. H., Gamen R., Arias J. I., Morrell N., Maíz Apellániz J., Alfaro E., Walborn N., Sota A., 2010, in Rivinius Th., Curé M., eds, Revista Mexicana de Astronomia y Astrofisica Conf. Ser. Vol. 38, The Interferometric View on Hot Stars, Revista Mexicana de Astronomia y Astrofisica, Mexico. p. 30
Barbá R. H., Gamen R., Arias J. I., Morrell N. I., 2017, in Eldridge J. J., Bray J. C., McClelland L. A. S., Xiao L., eds, Proc. IAU Symp. 329, The Lives and Death-Throes of Massive Stars, Cambridge University Press, Cambridge, p. 89
Bernstein R., Shectman S. A., Gunnels S. M., Mochnacki S., Athey A. E., 2003, in Iye M., Moorwood A. F. M., eds, Proc. SPIE Conf. Ser. Vol. 4841, Instrument Design and Performance for Optical/Infrared Ground-based Telescopes. SPIE, Bellingham, p. 1694
Conti P. S., Garmany C. D., Hutchings J. B., 1977, ApJ, 215, 561
Cox N. L. J. et al., 2017, A&A, 606, A76
Dekker H., D'Odorico S., Kaufer A., Delabre B., Kotzlowski H., 2000, in Iye M., Moorwood A. F., eds, Proc. SPIE Conf. Ser. Vol. 4008, Optical and IR Telescope Instrumentation and Detectors. SPIE, Bellingham, p. 534
Donati J.-F., Babel J., Harries T. J., Howarth I. D., Petit P., Semel M., 2002, MNRAS, 333, 55
Ekström S. et al., 2012, A&A, 537, A146
Fullerton A. W., Gies D. R., Bolton C. T., 1996, ApJS, 103, 475
Georgy C., Meynet G., Ekström S., Wade G. A., Petit V., Keszthelyi Z., Hirschi R., 2017, A&A, 599, L5
Grunhut J. H. et al., 2017, MNRAS, 465, 2432
Harries T. J., Howarth I. D., 1996, A&A, 310, 235
Hubrig S. et al., 2011, A&A, 528, A151
Humphreys R. M., 1978, ApJS, 38, 309
Hunter I., Smoker J. V., Keenan F. P., Ledoux C., Jehin E., Cabanac R., Melo C., Bagnulo S., 2006, MNRAS, 367, 1478
Langer N., 2012, ARA&A, 50, 107
Lindegren L., et al.. 2018, A&A, 616, A2
Mahy L., Hutsemékers D., Nazé Y., Royer P., Lebouteiller V., Waelkens C., 2017, A&A, 599, A61
Mel'Nik A. M., Dambis A. K., 2009, MNRAS, 400, 518
Morel T. et al., 2015, in Meynet G., Georgy C., Groh J., Stee P., eds, Proc. IAU Symp. Vol. 307, New Windows on Massive Stars, Cambridge University Press, Cambridge, p. 342
Nazé Y., Walborn N. R., Rauw G., Martins F., Pollock A. M. T., Bond H. E., 2008, AJ, 135, 1946
Nazé Y., ud-Doula A., Spano M., Rauw G., De Becker M., Walborn N. R., 2010, A&A, 520, A59
Nazé Y., Mahy L., Damerdji Y., Kobulnicky H. A., Pittard J. M., Parkin E. R., Absil O., Blomme R., 2012a, A&A, 546, A37
Nazé Y., Zhekov S. A., Walborn N. R., 2012b, ApJ, 746, 142
Nazé Y., Petit V., Rinbrand M., Cohen D., Owocki S., ud-Doula A., Wade G. A., 2014, ApJS, 215, 10
Nota A., Pasquali A., Drissen L., Leitherer C., Robert C., Moffat A. F. J., Schmutz W., 1996, ApJS, 102, 383
Petit V. et al., 2013, MNRAS, 429, 398
Petit V. et al., 2017, MNRAS, 466, 1052
Rauw G., Nazé Y., 2016, Adv. Space Res., 58, 761
Romero G. A., 2006, PhD thesis, Universidad Nacional de La Plata (Argentina)
Sana H. et al., 2014, ApJS, 215, 15
Silvester J., Wade G. A., Kochukhov O., Bagnulo S., Folsom C. P., Hanes D., 2012, MNRAS, 426, 1003
Smoker J. V., Keenan F. P., Fox A. J., 2015, A&A, 582, A59
Stibbs D. W. N., 1950, MNRAS, 110, 395
Tokovinin A., 1992, in McAlister H. A., Hartkopf W. I., eds, ASP Conf. Ser. Vol. 32, IAU Colloq. 135: Complementary Approaches to Double and Multiple Star Research. Astron. Soc. Pac., San Francisco, p. 573
Wade G. A. et al., 2012, MNRAS, 419, 2459
Wade G. A. et al., 2016, MNRAS, 456, 2
Wade G. A. MiMeS Collaboration, 2015, in Balega Y. Y., Romanyuk I. I., Kudryavtsev D. O., eds, ASP Conf. Ser. Vol. 494, Physics and Evolution of Magnetic and Related Stars. Astron. Soc. Pac., San Francisco, p. 30
Walborn N. R. et al., 2004, ApJ, 617, L61
Walborn N. R., 1972, AJ, 77, 312
Walborn N. R., 1973, AJ, 78, 1067
Walborn N. R., Sota A., Maíz Apellániz J., Alfaro E. J., Morrell N. I., Barbá R. H., Arias J. I., Gamen R. C., 2010, ApJ, 711, L143
Weisskopf M. C., O'dell S. L., van Speybroeck L. P., 1996, in Hoover R. B., Walker A. B., eds, Proc. SPIE Conf. Ser. Vol. 2805, Multilayer and Grazing Incidence X-Ray/EUV Optics III. SPIE, Bellingham, p. 2

This paper has been typeset from a TEX/LATEX file prepared by the author.